TRENDS IN SCIENCES 2025; 22(12): 10639
https://doi.org/10.48048/tis.2025.10639
RESEARCH ARTICLE

Selective Fluorescence Quenching Sensor for Trace Determination of Iron (Fe^{2+}/Fe^{3+}) in Water Sample Using Natural Carbon Dots (CDs) Synthesized by Microorganisms from Leech Lime (*Citrus hystrix* DC.) Fermentation Extract

Jirapat Janshongsawang[1], Nipaporn Pimsin[1], David Nugroho[2], Prawit Nuengmatcha[3,4], Paweena Porrawatkul[3] and Saksit Chanthai[1,*]

[1]*Materials Chemistry Research Center, Department of Chemistry and Center of Excellence for Innovation in Chemistry, Faculty of Science, Khon Kaen University, Khon Kaen 40002, Thailand*
[2]*Department of Integrated Science, Faculty of Science, Khon Kaen University, Khon Kaen 40002, Thailand*
[3]*Center of Excellence in Nanomaterials Chemistry, Department of Chemistry, Faculty of Science and Technology, Nakhon Si Thammarat Rajabhat University, Nakhon Si Thammarat 80280, Thailand*
[4]*Creative Innovation in Science and Technology, Faculty of Science and Technology, Nakhon Si Thammarat Rajabhat University, Nakhon Si Thammarat 80280, Thailand*

([*]Corresponding author's e-mail: sakcha2@kku.ac.th)

Received: 12 May 2025, Revised: 30 June 2025, Accepted: 18 July 2025, Published: 30 August 2025

Abstract

This study presents a green and low-cost fluorescence sensing platform for the simultaneous detection of Fe^{2+} and Fe^{3+} ions (total iron) in water using carbon dots (CDs) synthesized via natural fermentation of *Citrus hystrix DC.* (leech lime) fruit. The hypothesis is that functional groups on the surface of biosynthesized CDs can selectively coordinate with both iron oxidation states, resulting in effective fluorescence quenching. The CDs were characterized using UV-Vis spectroscopy, fluorescence spectroscopy, FTIR and TEM, confirming their spherical morphology and strong blue emission at 454 under 330 nm excitation. Experimental optimization was performed for key sensing parameters, including pH, ionic strength (NaCl), EDTA concentration, reaction time and temperature. Under optimized conditions (pH 4, 5 mM EDTA, 0.1 M NaCl, 50 °C, 10 min reaction), a linear fluorescence quenching response was observed in the 30 - 100 µM total iron range, with a limit of detection (LOD) of 8.05 µM and limit of quantification (LOQ) of 26.85 µM. The method demonstrated high selectivity toward iron ions over 20 other metal ions and negligible interference from chloride and carbonate. Recovery tests in drinking and tap water samples yielded values between 86.65% - 115.06%, validating the method's applicability for real-world water monitoring. This work highlights the potential of naturally derived CDs as effective and environmentally sustainable probes for trace iron analysis in environmental samples.

Keywords: Carbon dots, Graphene quantum dots, Fluorescence, Quenching effect, Leech lime extract, Metal ions

Introduction

Iron is widely known as the most abundant heavy metals, and in particular its inorganic species such as ferrous (Fe^{2+}) and ferric (Fe^{3+}) ions have significant roles in biological systems [1]. Both Fe^{2+} and Fe^{3+} are thus essential for several biological and chemical systems in living things, including an essential trace element in the human body, oxygen transport, metabolism storage, electron transfer in enzymatic reactions, improving immunity, forming hemoglobin, acting as an oxidation catalyst in oxidoreductase reactions and the chain of respiration in the mitochondria [2-4]. However, this metal has mostly two types of valence states: Fe^{2+} and Fe^{3+}, which constantly transform with each other, making it very hard to identify Fe^{2+} and Fe^{3+} ions independently [5]. Furthermore, the total concentrations of Fe^{2+} / Fe^{3+} ions

among the heavy metals are frequently discovered in environmental water, including drinking water and tap water. These amounts are an important consideration when evaluating the water quality in order to avoid any risks to the general population that may arise from the iron [2]. An excessive amount of iron in water has an impact on the nutritional chain, which causes organisms to accumulate such heavy metals. It has certain an impact on health, leading to several illnesses such as diabetes, heart disease and liver disease. As well, it raises the risk of hemochromatosis along with associated illnesses, including cancer [6]. In order to avoid the harmful consequences of excessive quantities of iron in the human body, it is significant to develop practical analytical methods that are precise, dependable and focused on investigating and utilizing techniques for measuring and tracking quantities of Fe^{2+} and Fe^{3+} ions [7]. At present, many analytical approaches have been performed for evaluating the quantity of Fe^{2+} and Fe^{3+} ions, for instance, UV-Visible spectrophotometry [8], colorimetric analysis [9], chemosensor [10], electrochemical sensing technology [11], fluorescent spectrophotometry [12] and dual-mode luminescence and colorimetric sensing [7]. There are plenty of research papers as well on the selective detection of heavy and transition metals by utilizing CDs as sensing probes [13,14].

Carbon dots (CDs), a new type of fluorescent carbon nanomaterials, have gained extensive research interest due to their fascinating properties [14]. Especially their great biological compatibility, low toxicity, environmental friendliness, fantastic photostability, high water solubility. They are extensively utilized in biomolecules detection, tiny organic particles, metal ions, anions and stable chemical features, making them powerful applications for novel varieties of fluorescent probes and overcoming the typical disadvantages of past fluorescent probes [15]. With diameters smaller than 10 nm were synthesized by utilizing carbon-containing substances as carbon sources. Also, they have been employed effectively because their physical and chemical characteristics are exactly like those of semiconductor graphene quantum dots (GQDs) [16]. At the present, there is an evidence of several distinct CDs preparation methods. In general, the CDs synthesis can be divided into two approaches: “top-down” and “bottom-up” [17]. Because the top-down process involves cutting and oxidation, the bigger carbon association structure is split toward small carbon nanoparticles, which produce the CDs products with reduced particle diameters. Conversely, in order to create nanoscale CDs, the method that is applied from the bottom up relies on a sequence of chemical reactions involving precursor molecules of small size [16]. The CDs could be generated through etching from large carbon-based materials, for example, graphite [18], carbon fibers [19] and biomass-derived activated carbon [20]. The treatment methods via hydrothermal [21] or microwave heating [22] of organic compounds like glycerol and urea [23], glucose [24] and citric acid [25] have been available. In addition, numerous works have been put forth into creating environmentally friendly synthetic processes for the CDs production. Biological wastes are used, which includes kitchen garbage, citrus fruit peels and green tea junk, as cheap and green materials sources [26]. Hence, leech lime fruit (*Citrus hystrix* DC.) is also suitable for being utilized carbon source to be CDs biosynthesized rather than chemical traditional methods.

Leech lime, formerly referred to Kaffir lime (*Citrus hysteria* or *Citrus hystrix*), is a member of the Ruta family plant (*Rutaceae*) [27]. There are other names for *Citrus hystrix* DC. as well, including “Makrut” (in Thai), kaffir lime and leech lime [28]. A citrus fruit is most commonly grown in Southeast and South Asian countries [29,30]. Both the fruit and the leaves that from the leech lime (Kaffir lime) are currently utilized in herbal treatments and cooking [31]. In addition, citric acid, which is an important organic acid, was reported to be a compound discovered in the citrus fruits [32]. So, the development of natural carbon dots (CDs) is subject for more potential uses.

In this study, the CDs existing its blue-emission as a source of carbon was obtained from simple fermented extraction of leech lime fruit (*Citrus hystrix* DC.). Since leech lime fruit is non-toxic, cheap and large quantity, the CDs are applied as fluorescence sensor for trace detection of total iron (Fe^{2+} and Fe^{3+}). The use of natural carbon dots (CDs) as fluorescence sensors for the simultaneous detection of Fe^{2+} and Fe^{3+} ions represent a novel and targeted approach. This strategy emphasizes the sensor's performance over the individual detection of specific iron species. To date, only a limited number of studies have reported the high-selectivity detection of

both Fe^{2+} and Fe^{3+}or total iron in complex water matrices such as drinking water and tap water.

Materials and methods

Plant material and chemicals

Leech lime fruit (*Citrus hystrix* DC.) was used as a raw herb material to produce its natural fermented extract. It is available in local fresh markets in Khon Kaen province, Thailand. All of chemicals used were of analytical grade. Ethylenediaminetetraacetic acid (EDTA) was purchased from Ajex Finechem (Australia). Iron(II) sulfate heptahydrate, iron(III) chloride hexahydrate, citric acid and boric acid (QRec, New Zealand), sodium chloride (BDH, England), acetic acid, sodium hydroxide, ortho-phosphoric acid (RCI Labscan, Thailand) were also used. Deionized water (Simplicity Water Purification System, Model Simplicity 185, Millipore, U.S.A) was used throughout the experiments.

Instruments

Fluorescence spectrum and intensity was mainly obtained from a Shimadzu RF-5301PC spectrofluorophotometer (Japan) with an excitation and emission slit width of 3 - 5 nm. UV-Visible spectrophotometer (Agilent, Germany), model number 8,453 was used. A quartz cell with a path length of one centimeter (Fisher Scientific, U.S.A.), an analytical balance (Model LX 220A, Precisa, Thailand), an ultrasonic cleaner (Model VGT-2300, GT SONIC, Hong Kong) and a pH meter (UB-10 UltraBasic, Denver, USA) were also used utilized. A Fourier transform infrared spectrometer from Bruker (TENSOR27), Germany was used to measure attenuated total reflectance-Fourier transform infrared (ATR-FTIR) spectroscopically. The morphology, size and shape of the obtained carbon dots was evaluated by transmission electron microscopy (TEM) (TEM, JEOL, JEM-2010, Japan) operated at an acceleration voltage of 200 kV.

Preparation of carbon dots (CDs)

The obtained carbon dots (CDs) were slowly formed via a natural fermentation process at ambient temperature, the so-called the fermented extract of leech lime fruit (*Citrus hystrix* DC.). The extract part was finely filtered using a cartridge syringe with a diameter of 0.22 μm filter membrane. The clear extract solution is then diluted with deionized water as stock CDs sample kept in refrigerator (4 °C) prior to experiments. Practically, the CDs nanoparticles was homogeneously dispersed in aqueous solution at different diluted concentrations and relatively stable in room temperature after timely adjusted by its absorbance and fluorescence intensity.

Optical properties of the CDs

The UV-Visible absorption of the CDs was measured in comparison with that of GQDs. Also, its fluorescence spectrum of the CDs was acquired via maximum excitation wavelength and maximum emission wavelength with appropriate slit width of 3 - 5 nm. Furthermore, ATR-FTIR of the CDs vs GQDs were carried out to identify their specific chemical structure and compared.

Morphology images of the CDs by HR-TEM

The morphological images of both CDs and GQDs were comparatively demonstrated by transmission electron microscopy (TEM) to confine their nanoparticle dispersion and particle size as well.

Selective fluorescence quenching effect of CDs by various metal ions

The selective fluorescence quenching effect of CDs was investigated by various metal ions. As a typical procedure, 40 μL aliquot of the CDs obtained from the fermented extract of leech lime (*Citrus hystrix* DC.) was filtered with a 0.22 μm filter membrane, added 1 mL of 1 mM EDTA and adjusted with deionized water to 10 mL final volume solution used as a blank. For screening test of various metal ions, each 1 mL of 0.5 mM metal ions solution, including Cr^{3+}, Cu^{2+}, Zn^{2+}, Mg^{2+}, Fe^{2+}, Cr^{6+}, Ni^{2+}, Co^{2+}, Fe^{3+}, Mn^{2+}, Cd^{2+}, Pb^{2+}, Li^{+}, Na^{+}, K^{+}, Ca^{2+}, Ba^{2+}, Al^{3+}, As^{5+}, As^{3+}, Ag^{+} and Hg^{2+} was added into the mixture of the blank sample and also adjusted to 10-mL final volume with deionized water. Then, their fluorescence intensities were recorded at the excitation and emission wavelengths of 330 and 454 nm, respectively, with its excitation/emission slit width of 3/3 nm. Each of the experiments was conducted under the same conditions at room temperature.

Optimization conditions for Fe^{2+}/Fe^{3+} mixed ions

The trace determination of Fe^{2+}/ Fe^{3+} was carried out using dilute solution of CDs at room temperature with 1 mM of EDTA as an auxiliary complexing medium. The both kinds of the iron hydrate ($FeSO_4•7H_2O$ and $FeCl_3•6H_2O$) were used for the standard stock solution of Fe^{2+} and Fe^{3+}. To study of both sensitivity and selectivity of the fluorescence quenching sensor for the mixed fraction of Fe^{2+}/Fe^{3+} with different concentration, the following solution included the addition of 0.1 M NaCl and 5 mM EDTA into the CDs solution (200 µL) then adjusted with Britton-Robinson buffer at pH 4 under the optimum condition. Following, their assigned different concentration ratios of total Fe^{2+}/Fe^{3+} ions at 10, 20, 40, 60, 80 and 100 µM were added into the reaction mixture in a 10-mL volumetric flask. After heating at 50 °C for 10 min in an ultrasonic water bath, the mixed solution was allowed to cool to room temperature (~25 °C), after which fluorescence measurements were recorded at an emission wavelength of 454 nm (λ_{ex} = 330 nm).

Method validation

Evaluation of an analytical method's quality is consistently assessed based on its appropriateness for the intended purpose, recovery capability, need for standardization, sensitivity, stability of the analyte, ease of analysis, necessary skill set, as well as time and cost considerations, in that particular sequence. It is of utmost importance to rigorously ascertain, via a systematic procedure, the suitability of the analytical method in question for its intended objective.

Linearity, LOD and LOQ

Linearity is necessary analytical factor for trace determination of such target ions, in particular for wide range of their calibration curve. This is also to identify how its sensitivity of the developed method. The determination of the limit of detection (LOD), limit of quantitation (LOQ) are critical parameters in method validation within the field of analytical chemistry. Both LOD and LOQ are utilized to characterize the minimum concentration of an analyte that can be accurately determined by an analytical method. In this study, the determination of the LOD is performed using the formula LOD = 3SD/S, while the LOQ is calculated using the formula LOQ = 10SD/S. In these calculations, SD denotes the standard deviation of the blank readings multiplied by three and S indicates the slope of the linear regression plot.

Recovery study

The percentage recovery (% Recovery) is employed to ascertain the proportion of the original material that is obtained following the completion of a chemical reaction. The calculation of recovery has been performed using the formula % Recovery = C_{found} / C_{added}×100. In this context, C_{found} denotes the concentration of the analyte subsequent to the introduction of a known quantity of standard into the actual sample. C_{added} signifies the concentration of the analyte inside the actual sample, while C_{added} reflects the concentration of the known quantity of standard that was introduced into the actual sample.

Trace determination of total iron in real water sample

Total iron model was determined to evaluate the practical use of the developed method in real water samples five drinking water samples and two tap water samples, using the CDs as fluorescence quenching sensor. The drinking water samples were collected from the general retail stores. Tap water samples were received from the dormitory of Khon Kean University and laboratory which were kept with 1% (v/v) dilute nitric acid to stop any bacterial activity in plastic bottles. The reaction mixture was prepared by using 200 µL CDs solution, 1 mL 0.1 M NaCl, 1 mL 5 mM EDTA and 1 mL water sample and then adjusting with buffer solution pH 4 in a 10 mL final volume under 50 °C for 10 min using ultrasonic bath prior to analysis by fluorescence spectrophotometer.

Results and discussion

Characterization of CDs by FTIR

The water extract drawn from leech lime (*Citrus hystrix* DC.) fermentation tank was used as the main source of natural carbon dots (CDs). To determine which chemical functional groups on the CDs surface, FTIR spectrum was acquired. According to **Figure 1**, it exhibits the characteristic absorption broad band at 3,257 cm^{-1} and the small band at 2,930 cm^{-1} were assigned to the stretching vibrations of the O-H

(hydroxyl) and C-H bonds, respectively [33]. The stretching vibrations of C=O (carbonyl) were identified as the cause of the peak at 1,776 cm^{-1}. The characteristic peak at 1,610 cm^{-1} was assigned to the stretching vibration absorption in the strong region corresponding to the aromatic containing function group of the C=C bond, and the peak at 1,022 cm^{-1} implied the existence of C-O stretching vibration [34,35]. The CDs are very easily soluble in water due to the presence of hydroxy functional groups on their surface, as indicated by the FTIR absorption peaks [36]. While the bands in the range of 1,449 cm^{-1} were assigned to the C-H group of bending vibrations of benzene [37], the bands at 820 cm^{-1} were assigned to the C-H bending vibration (out-of-plane) [31]. The spectra of CDs were similar and confirmed the frequency of these functional groups by comparing with those of GQDs.

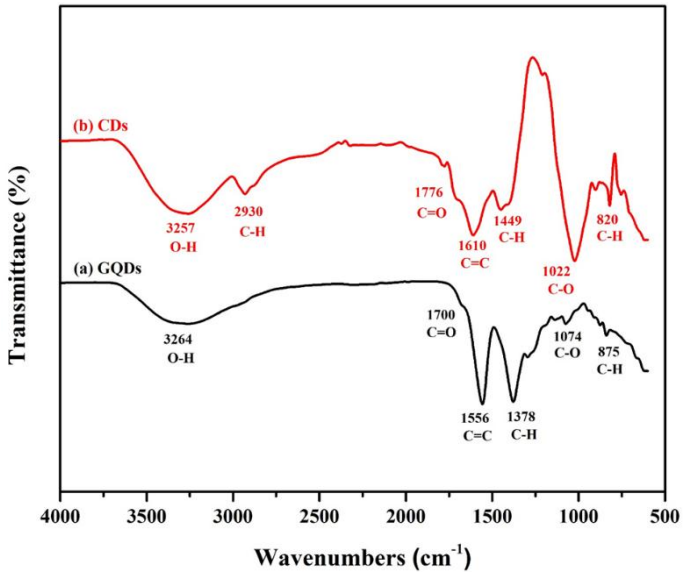

Figure 1 The FTIR spectra of (a) GQDs and (b) CDs.

Characterization of CDs by TEM

When examining the morphology, size and shape of nanomaterials, such as carbon dots (CDs) and graphene quantum dots (GQDs), transmission electron microscopy (TEM) is a potent technique. TEM pictures (**Figure 2**) show that, although being carbon-based nanomaterials, CDs and GQDs differ structurally. Most CDs are either quasi-spherical or spherical. CDs are typically between 1 and 10 nm in size. TEM images may reveal that CDs have a propensity to combine and form clusters. The surface functional groups of CDs can vary, which could impact TEM picture contrast. GQDs range in size from 2 to 20 nm and they frequently appear as tiny flakes. In comparison to CDs, GQDs are typically smaller and have a more defined, planar structure. Graphitic layers are represented by the distinct crystalline structure and observable lattice fringes of GQDs. In TEM images, different layers or sheets can be seen due to the planar nature of GQDs, which can also aggregate. To summarize, TEM images of GQDs will reveal compact, planar structures with distinct crystalline patterns and lattice fringes, whereas TEM photos of CDs will typically show spherical particles with a maybe less obvious interior structure.

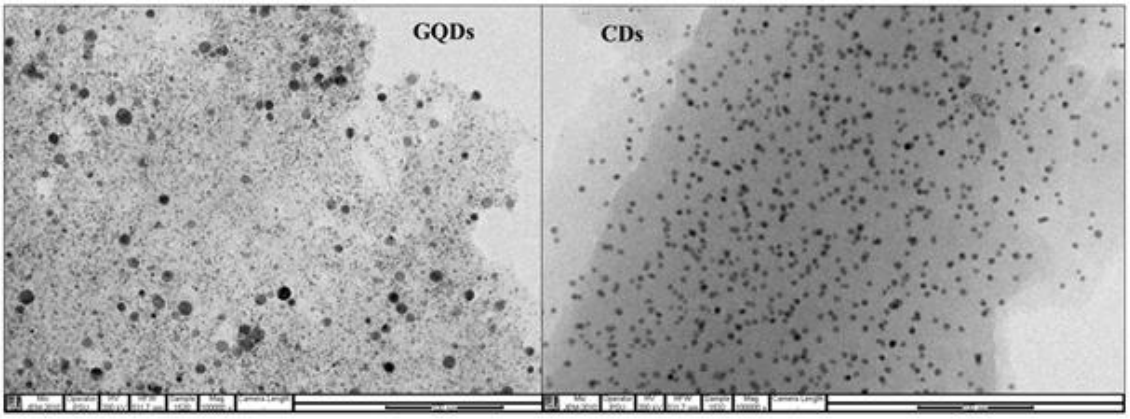

Figure 2 TEM images of GQDs and CDs.

UV-Visible absorption and fluorescence properties

The UV-Visible absorption spectra of carbon dots (CDs) and graphene quantum dots (GQDs) dispersion in an aqueous solution were investigated to reveal the optical characteristics of the carbon nanoparticles. As exhibited in **Figure 3**, the CDs (red line) have a relatively low UV absorption spectrum band ranged from 250 to 400 nm, which is occasionally visible in the UV-Vis spectrum. Also, the GQDs (black line) have a UV absorption maximum at 370 nm, which was quite low and attributable to the n-π* transition came from the carbonyl double bond as previously demonstrated for GQDs [38].

Also from the fluorescence results, their excitation and emission spectra of both CDs compared with GQDs, as shown in **Figure 3(a)**, reveal the maximum peak emission wavelength of CDs at 454 nm, followed by the excitation wavelength at 330 nm. While, GQDs display its spectra of the excitation and emission wavelengths at 370 and 460 nm (**Figure 3(b)**), respectively. Thus, when compare their highest emission peaks between CDs and GQDs, the CDs gives an excellent emission, stronger than that of GQDs. **Figure 3(c)** shows that the color solution of GQDs and CDs in an aqueous solution is lightly yellow under visible light, but blue under UV light as demonstrated in **Figure 3(d)**.

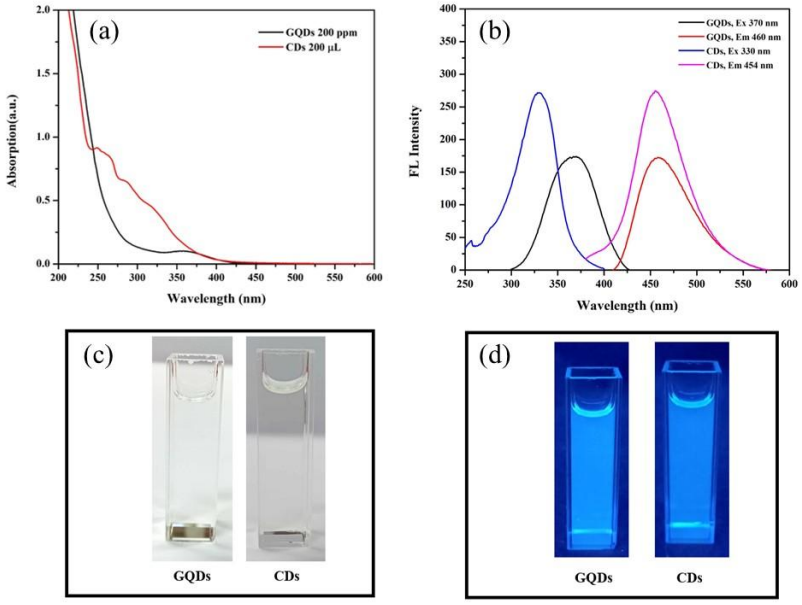

Figure 3 (a) UV-Vis absorption spectra of GQDs and CDs at 50-fold dilution (200 µL in 10 mL water); (b) Fluorescence spectra of GQDs and CDs at the same dilution; $\lambda_{ex}/\lambda_{em}$ = 370/460 nm for GQDs and 330/454 nm for CDs (slit width 3/3 nm); (c) visible-light image and (d) UV-light image of GQDs and CDs aqueous solutions under identical conditions.

Effect of CDs on the selectivity of Fe^{2+}/Fe^{3+} ions

Selective fluorescence quenching by various metal ions

To examine the interaction between CDs and Fe^{2+} and Fe^{3+}, its selectivity was studied in details. Various metal ions, including Cr^{3+}, Cu^{2+}, Zn^{2+}, Mg^{2+}, Fe^{2+}, Cr^{6+}, Ni^{2+}, Co^{2+}, Fe^{3+}, Mn^{2+}, Cd^{2+}, Pb^{2+}, Li^{+}, Na^{+}, K^{+}, Ca^{2+}, Ba^{2+}, Al^{3+}, As^{5+}, As^{3+}, Ag^{+} and Hg^{2+}, were used to investigate their selectivity under the same conditions as done with both Fe^{2+} and Fe^{3+}. According to **Figure 4**, it is evident that only Fe^{2+} and Fe^{3+} have a significantly quenched effect at 454 nm, as the emission intensities of the other metal ions show no discernible changes. This indicates that both Fe^{2+} and Fe^{3+} ions have a high potential selectivity for CDs in comparison to other metals. Consequently, Fo–F value, where Fo and F are the fluorescence intensities of CDs without metal ions and that containing various metal ions, provides an obvious instance of the quenching effects of the Fe^{2+} and Fe^{3+} ions [33].

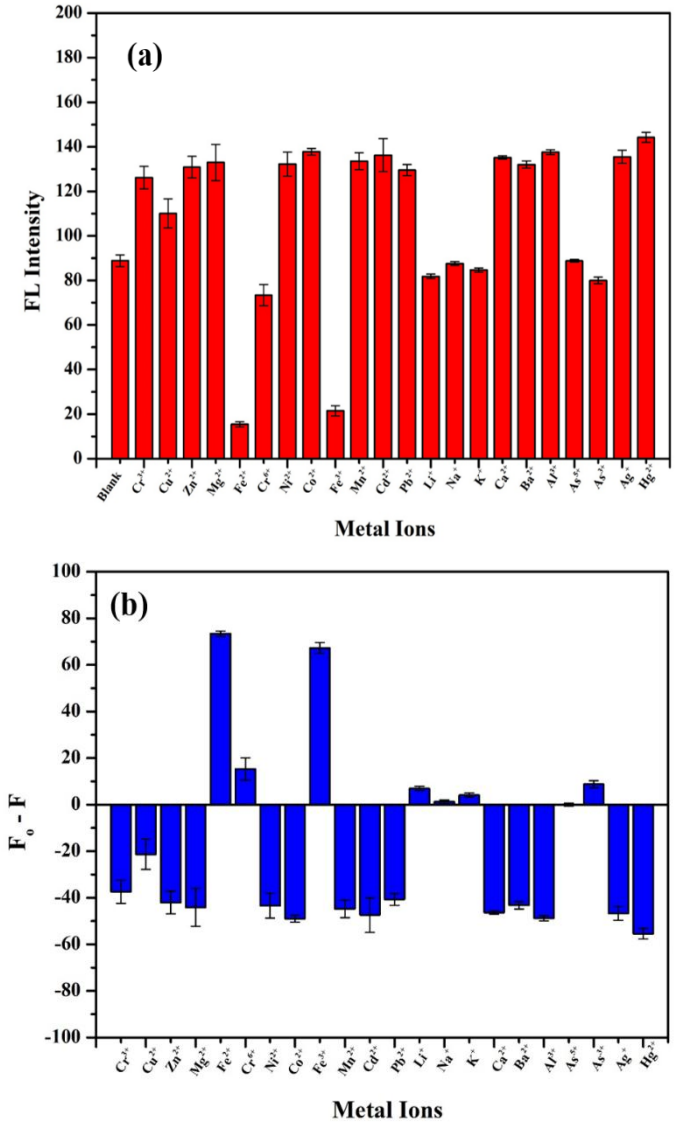

Figure 4 The comparison in (a) fluorescent intensities of CDs between its blank (Fo) and in the presence of different metal ions (F) and (b) the Fo - F values of CDs response the quenching effect of these metal ions. (The volume and concentration of CDs, EDTA and metal ions were 40 μL, 1 mM and 0.5 mM, respectively; the fluorescence was recorded at 454 nm. Excitation wavelength was 330 nm).

Effect of suitable based concentration of the CDs extract

Fluorescence intensity was used to estimate the effect of CDs concentration. As a result, the amounts of CDs required to monitor their complex interactions of Fe^{2+} and Fe^{3+} are shown in **Figure 5**, which is definitely very high and significant at a diluted solution of the CDs about 50 folds (200 µL). Thus, it was a choice to evaluate the fluorescence quenching effect of both Fe^{2+} and Fe^{3+} using a 50-fold dilution of the CDs extract for further experiments.

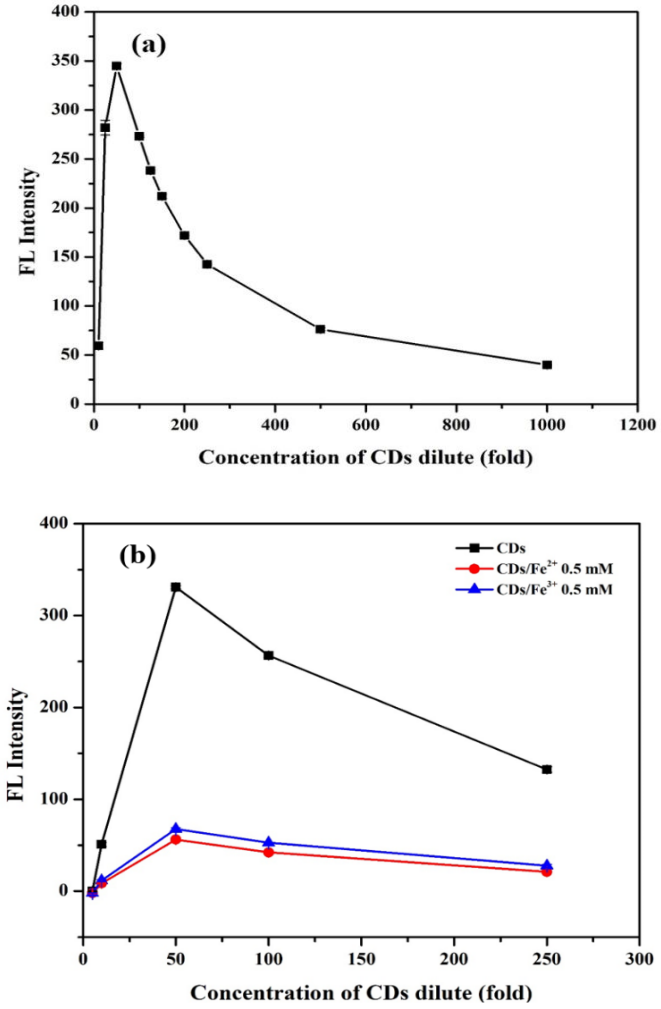

Figure 5 (a) Fluorescence (FL) intensities of various concentrations of the CDs expressed as its dilution from 10 to 1000 folds and (b) the quenching effect of CDs in the presence of 0.5 mM of Fe^{2+} and Fe^{3+} at $\lambda_{ex}/\lambda_{em}$ = 330/454 nm, slit width 3/3.

Effect of each concentration of Fe^{2+} and Fe^{3+} ions

The effectiveness of Fe^{2+} and Fe^{3+} detection is confirmed by the fluorescence spectra of CDs with various concentrations of Fe^{2+} and Fe^{3+} ions, as shown in **Figure 6** [39]. These spectra present a gradual decrease in CD fluorescence with an increase in Fe^{2+} and Fe^{3+} concentrations, as indicated in **Figures 6(a)** and **6(b)** [33]. According to **Figure 6(c)**, the comparison of the Fo -F quenching efficiencies of CDs in the presence of different amounts of Fe^{2+} and Fe^{3+} in the CDs solution is also given [24,34]. For the relationship between Fe^{2+} and Fe^{3+}, the parallel linear equations of both of lines with nearly identical slope values are presented to demonstrate the fluorescence quenching ability. This indicates that the fluorescence response of CDs media complexed with Fe^{2+} and Fe^{3+} was the same.

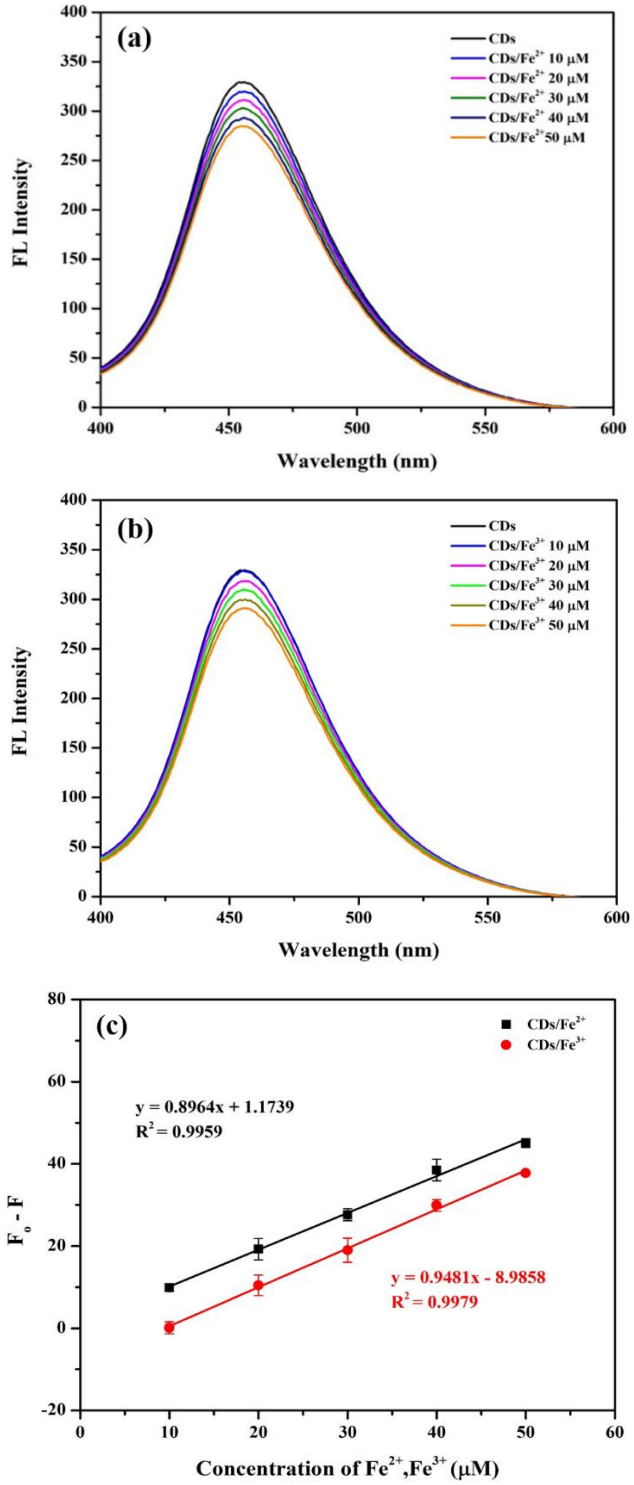

Figure 6 FL spectra of CDs resolved with (a) Fe^{2+} ions and (b) Fe^{3+} ions at different concentrations (10 - 50 µM). (c) Linear regression plots of fluorescence quenching response (Fo - F) of carbon dots toward Fe^{2+}, Fe^{3+} and total Fe (Fe^{2+}/Fe^{3+}) within the concentration range of 10 - 100 µM under optimized conditions (pH 4, 5 mM EDTA, 0.1 M NaCl, 50 °C, 10 min).

Effect of pH solution

The effect of pH solution on the fluorescence quenching of CDs by Fe^{2+} and Fe^{3+} was also studied, as shown in **Figure 7**. The findings suggest that the FL intensities of CDs were higher at pH 4 [34] and the difference in the fluorescence quenching of Fe^{2+} and Fe^{3+} was also more significant at this pH than that of other pH values. These results seem to demonstrate that

the FL intensity of CDs dispersed in the acid medium is stronger than that of the alkaline medium and the FL intensity gives the highest level at pH 4. Our work, thus, confirms that the as-prepared CDs have pH dependence because we were able to change the FL intensity by changing the pH value of the CDs solution [35]. Hence, the following studies were better set to concentrate on this optimal pH effect.

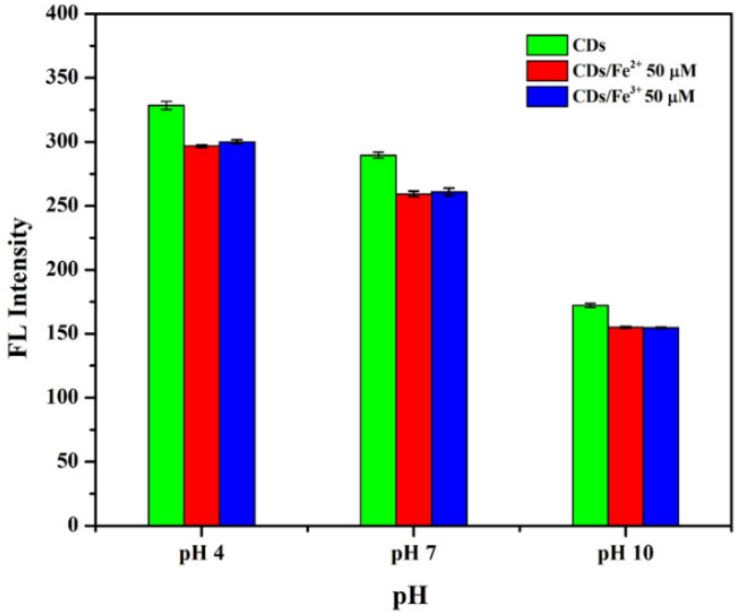

Figure 7 Effect of solution pH (pH 4, 7 and 10) on each 50 µM of either Fe^{2+} or Fe^{3+} ions detection

Effect of NaCl used as an ionic strength

The impact of an ionic strength on the stability of the CDs used in a solution of 0.1 M Britton-Robinson buffer (pH 4) containing various NaCl concentrations was additionally evaluated in this study as well. Their FL intensities remain stable as the ionic strength increases, as seen in **Figure 8**. The CDs were rather exhibited a residual charged surface, so there was barely any ionization of the functional groups of the carbon atoms on the surface of the CDs. Based on the results presented above, there is evidenced that the CDs were extraordinarily stable even dispersing under stressful solution conditions [38,40].

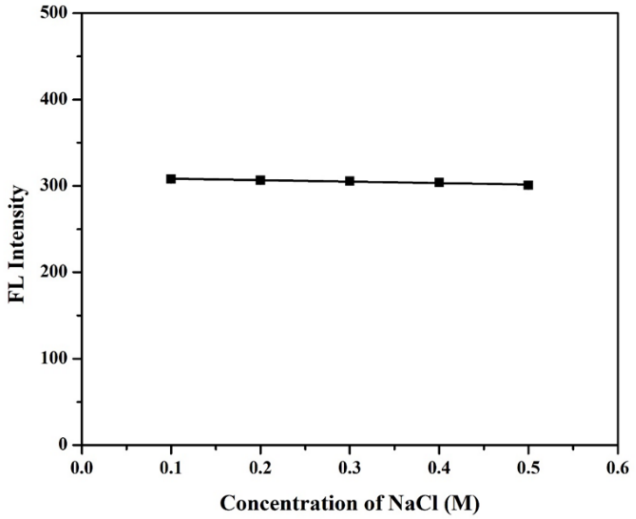

Figure 8 Effect of an ionic strength as using 0.1 - 0.5 M NaCl on the fluorescence quenching effect of total Fe ion (Fe^{2+}/Fe^{3+}).

Effect of EDTA as a general masking agent

In such case, this study was to investigate the effect of EDTA as a general masking agent for heavy metal ions when an aqueous sample was included. Different concentrations of EDTA at 1, 5, 10, 25, 50, 100 and 200 mM were added into CDs (200 µL), 0.1 M of NaCl and 50 µM of total iron (Fe^{2+}/Fe^{3+}) aqueous solution, which was adjusted to 10.0 mL in a volumetric flask before the fluorescence measurement. The F_o-F fluorescence intensity was monitored and presented, as shown in **Figure 9**. Following these results, there was a slight increase in the reaction mixture between total iron (Fe^{2+}/Fe^{3+}) and the CDs in the 5 - 25 mM range when the amount of EDTA increased. Then the F_o-F values remained constant after that. Based on the optimization study, 5 mM EDTA was selected as an effective masking agent to stabilize the iron ions and enhance the fluorescence quenching response during the sensing process.

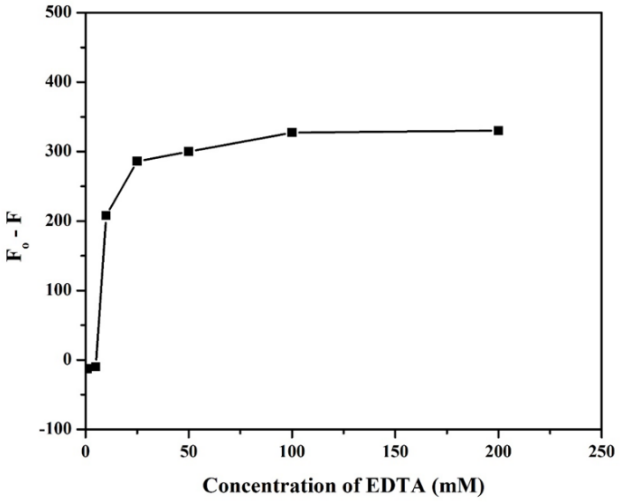

Figure 9 Effect of EDTA concentration (mM) containing 200 µL CDs and 0.1 M NaCl in Britton Robinson buffer solution at pH 4

Effect of the reaction time

The impact of the reaction time between total iron (Fe^{2+}/Fe^{3+}) and the CDs at various time intervals was also investigated at 10, 30, 40, 50 and 60 min. The results of the reaction time as shown in **Figure 10** were not affected significantly while the time increased continuously, confirming the excellent stability of the reaction mixture [35,38]. Because of this, it was chosen to concentrate at about 10 min in the following studies.

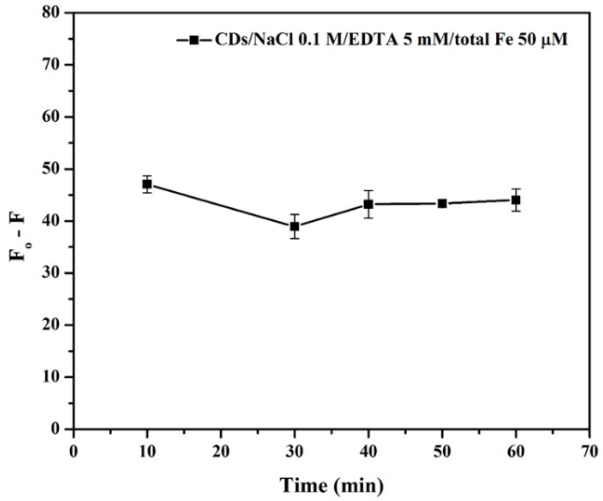

Figure 10 Effect of the variation reaction time (10 - 60 min) on total Fe ions detection.

Effect of the reaction temperature

The effect of reaction temperature was studied ranging from 25, 30, 40, 50 and 60 °C on both total iron (Fe^{2+}/Fe^{3+}) and the CDs used. Based on these heating effects, the net fluorescence F_o-F was observed and demonstrated in **Figure 11**, showing that the Fo-F increased and reached a maximum at 50 °C while the reaction temperature was increased continuously. Therefore, it was decided to settle at 50 °C for the subsequent experiments.

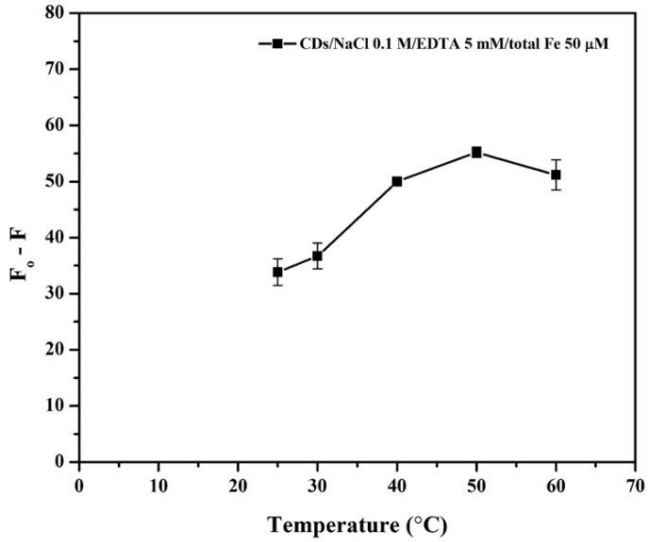

Figure 11 Effect of different reaction temperature (25 - 60 ℃) on total Fe ions detection.

Method validation

To assess the analytical performance of the proposed fluorescence quenching sensor for total iron (Fe^{2+}/Fe^{3+}) detection, a comprehensive method validation was conducted. The validation included linearity, limit of detection (LOD), limit of quantification (LOQ), precision, recovery and selectivity. Under the optimum conditions, total iron (Fe^{2+}/Fe^{3+}) in an aqueous solution can be analytically identified by the fluorescence quenching of the intact CDs. The combined fraction experiments of Fe^{2+}/Fe^{3+} were subject to generate the fluorescence spectra of CDs, which were subsequently applied to improve on the relationship between Fe^{2+}/Fe^{3+} concentration ratios and the fluorescence intensity of the CDs. The fluorescence spectra of CDs adaptation as various concentrations of total iron (Fe^{2+}/Fe^{3+}) are observed, as illustrated in **Figure 12(a)**. The fluorescence of the CDs is quenched at regular intervals and sensitive to both kinds of iron ions as the ion concentration increases. According to **Figure 12(b)**, there is a good linear correlation between the quenching efficiency ($y = 0.8232x + 6.0275$; $R^2 = 0.9959$) and the low concentration of total iron (Fe^{2+}/Fe^{3+}) with linear range of 10 - 100 µM. The linear equation (F_o-F) was used to calculate the quenching efficiency of total iron (Fe^{2+}/Fe^{3+}) where Fo is the fluorescence intensity of the blank and F is the fluorescence intensity with added different metal ion concentrations, respectively [37].

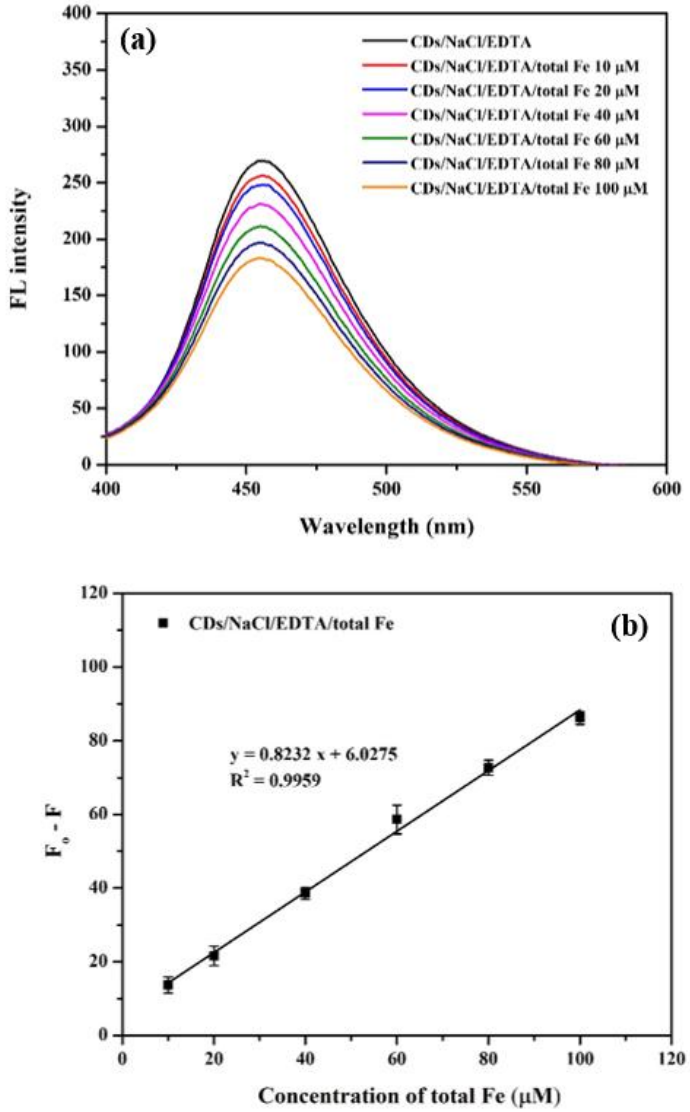

Figure 12 (a) The fluorescence spectra of the CDs at different concentrations of total Fe ions; (b) the corresponding linear calibration plots between Fo-F vs. concentrations of total Fe ions as their working range. The detection was performed under the optimized conditions of 200 µL CDs, NaCl 0.1 M, EDTA 5 mM in Britton Robinson buffer solution at pH 4 and heating under ultrasonic bath at 50 °C for 10 min.

The limits of detection (LOD) and limit of quantification (LOQ) were calculated with the corresponding equations: LOD = 3SD/S and LOQ = 10SD/S, where SD is the standard deviation for the 3 times of blank readings and S is the slope of a linear regression plot. **Table 1** provides a summary of the LOD, LOQ and calibration curve computations. The findings of linear range for trace determination of total iron (Fe^{2+}/Fe^{3+}) detection concentration range of 10 - 100 µM (LOD = 8.05 µM, LOQ = 26.85 µM). In addition to high efficiency and simultaneous detection of total iron on their universal curve, the interactions within total iron (Fe^{2+}/Fe^{3+}) and the CDs are expected to trigger the formation of nanoparticle complexes and the stiff structure's propensity to form stable heavy metal complexes. The present study is one of the few that can detect both Fe^{2+} and Fe^{3+} because it is interesting that very few publications have reported that the CDs can detect two types of iron ions simultaneously. When compared to a subset of pertinent reports of Fe^{2+} or Fe^{3+} trace detection by a variety of materials, for instance NCDs, N-CQDs, N, S-PPI-CDs and N, P-CQDs, as indicated in **Table 2,** this study shows that the proposed method can pave the way of this CDs media for total iron (Fe^{2+}/Fe^{3+}) detection with quite low LOD of 8.05 µM.

Table 1 Calibration curve, limit of detection (LOD), limit of quantitation (LOQ) of the method validation for total Fe^{2+}/Fe^{3+} fraction using fluorescence quenching sensor.

Calibration curve (µM)	Linear equations	R^2	LOD (µM)	LOQ (µM)
10 - 100	y = 0.82x + 6.03	0.9959	8.05	26.85

Table 2 Comparison of different fluorescence sensor for the detection of Fe^{2+}/Fe^{3+} using CDs probe.

Material	Synthetic sources	Synthetic method	Quantum yield	Sample types	Analyte	Linear range (µM)	LOD (µM)	Ref.
NCDs	citric acid	pyrolysis	65.5%	river water, lake water, tap water	Fe^{3+}	0 - 400	0.703	[1]
N-C dots	melamine	one-step neutralization heat reaction	12.8%	blood, tap water	Fe^{2+}, Fe^{3+}	0.01 - 10 and 0.02 - 10	0.005 and 0.0075	[5]
CDs	citric acid, polyvinyl pyrrolidone	hydrothermal method	30.21%	fluorescent ink	Fe^{3+}	0 - 300	0.0455	[35]
CDs (CA+Phen)	1,10-Phenanthroline, citric acid	solid state method	54%	milk	Fe^{2+}, Fe^{3+}	0 - 32 and 0 - 50	0.02 and 0.035	[42]
CDs	black tea	hydrothermal method	-	human serum	Fe^{3+}	0.25 - 60	0.25	[43]
N-CQDs	chitosan	hydrothermal method	-	tap water, lake water	Fe^{3+}	0 - 200	0.15	[44]
N,P-CQDs	amino trimethylene phosphonic acid (ATMP), sodium citrate	hydrothermal method	54%	river water, tap water	Fe^{2+}, Fe^{3+}	0 - 600 and 0 - 250	0.298 and 0.447	[45]
N,S-PPI-CDs	peanut protein isolate, cysteamine	hydrothermal method	-	drinking water	Fe^{2+}, Fe^{3+}	0 - 2	0.12 and 0.17	[46]
DA-S,N-CDs	citric acid, thiourea, dopamine	hydrothermal method	-	tap-water, lake-water	Fe^{2+}, Fe^{3+}	5 - 300 and 5 - 200	2.06 and 2.86	[47]
CDs	leech lime fruit (*Citrus hystrix* DC.).	natural fermentation process	-	drinking water	[a] Fe^{2+}/Fe^{3+}	10 - 100	8.05	This work

[a]Total Fe (Fe^{2+}: Fe^{3+})

In addition, their repeatability of precision was assessed using the relative standard deviation (RSD). **Table 3** describes the reproducibility (inter-day precision, the research performed over n = 5×3 successive days) and repeatability (intra-day precision, n = 3×3) of the linear regression slopes during working ranges from the purposed determining the presence of total iron (Fe^{2+}/Fe^{3+}) under such acceptable conditions. The optimal settings for chemicals, CDs fermented extract from leech lime, reaction temperature, and reaction time are presented in **Table 4** for the purposed detecting trace iron (Fe^{2+}/Fe^{3+}) in drinking water and tap water samples.

Table 3 RSD (%) of their slops from the intra-day and inter-day analysis calibration curve.

Calibration No.	Intra-day analysis[a]	Inter-day analysis[b]
	Linear equation	Linear equation
1	y = 0.7865x + 1.3465	y = 0.7008x + 13.4043
2	y = 0.8580x + 4.2439	y = 0.7483x + 3.9141
3	y = 0.8718x + 4.9705	y = 0.8118x + 6.1211
4		y = 0.7303x – 0.1570
5		y = 0.7772x + 9.5303
RSD (%)	5.46	5.67

[a] n = 3, [b] n = 5. RSD: relative standard deviation

Table 4 The optimum conditions to determine total Fe in the real water samples.

Parameter	Analytical data
Amount of CDs fermentation extract (μL)	200
NaCl concentration (mM)	100
EDTA concentration (mM)	5
pH value (Britton-Robinson buffer solution)	4.0
Reaction temperature under ultrasonic bath (˚C)	50
Reaction time under ultrasonic bath (min)	10

Trace analysis of total iron in real water sample

The developed fluorescence process was also employed for detecting trace analysis of total iron (Fe^{2+}/Fe^{3+}) in real water samples under suitable application conditions. Fluorescence sensing quenchers were then used to detect the total iron (Fe^{2+}/Fe^{3+}) in multiple sample matrices, for instance, drinking water and tap water. Evaluating the outcome of the recovery discovered with those water samples allowed us to definitively verify the accuracy of the method. Recoveries were calculated using spiked fractions of total iron (Fe^{2+}/Fe^{3+}) in drinking and tap water samples at three different concentrations (20, 40 and 60 μM) of the Fe^{2+}/Fe^{3+} standard solutions of interest [41]. The corresponding percentage of that recovery after being spiked had been calculated by using the previous equation: % Recovery = $[C_{found} / C_{added}]\times100$, where C_{found} represents the concentration of the analyte after adding a known amount of standard to the actual sample and C_{added} represents the concentration of the known amount of standard that was added to the real sample. These resulted outcomes are concluded in **Table 5**.

Table 5 Recovery results of the determination of total Fe in the real water samples by using the CDs as fluorescence sensing quenchers (X ± SD, n = 3).

Samples	Total Fe added (μM)	Total Fe found (μM)	Recovery (%)
Drinking water samples 1	0	-	-
	20	22.67 ± 0.73	113.35
	40	39.60 ± 1.06	98.98
	60	60.43 ± 1.31	100.72

Samples	Total Fe added (µM)	Total Fe found (µM)	Recovery (%)
Drinking water samples 2	0	-	-
	20	17.33 ± 2.39	86.65
	40	41.72 ± 1.51	104.29
	60	62.91 ± 2.11	104.85
Drinking water samples 3	0	-	-
	20	18.05 ± 1.47	90.25
	40	39.75 ± 1.80	99.37
	60	60.25 ± 0.80	100.41
Drinking water samples 4	0	-	-
	20	19.18 ± 2.63	95.89
	40	37.26 ± 0.17	93.14
	60	64.45 ± 1.41	107.42
Drinking water samples 5	0	-	-
	20	21.48 ± 1.10	107.38
	40	43.47 ± 0.85	108.68
	60	66.95 ± 0.55	111.59
Tap water 1	0	-	-
	20	18.57 ± 0.72	92.85
	40	41.49 ± 1.03	103.71
	60	69.04 ± 0.88	115.06
Tap water 2	0	-	-
	20	19.50 ± 2.29	97.49
	40	44.38 ± 1.76	110.96
	60	65.12 ± 0.54	108.53

- not detect

Conclusions

In this study, a standard calibration curve was successfully optimized for the fluorescence quenching sensor, using the CDs extracted from natural fermentation of leech lime (*Citrus hystrix* DC.), for iron detection. So, the use of CDs as a simple sensor is the novel discovery applied for the two Fe^{2+}/Fe^{3+} ions. The CDs was characterized by spectroscopic techniques including fluorescence spectroscopy, UV-Visible spectroscopy and FTIR and TEM image analysis. The CDs sensing probe is stable, sensitive and effective for total iron detection under optimized conditions. There was an excellent linear relationship between the fluorescence intensity of the CDs and the total iron (Fe^{2+}/Fe^{3+}) concentrations in the range of 10 - 100 µM, with 8.05 µM LOD and 26.85 µM LOQ. Therefore, the developed method demonstrated much satisfactorily recovery for of the total iron determination in tap water (92.85% - 115.06%) and drinking water (86.65% - 113.35%) samples.

Acknowledgements

The authors thank Materials Chemistry Research Center (MCRC) and Center of Excellence for Innovation in Chemistry (PERCH-CIC), Department of Chemistry, Faculty of Science, Khon Kaen University Consortium, Khon Kaen, Thailand for financial support.

Declaration of Generative AI in Scientific Writing

The authors' own intellectual contributions were not replaced, nor were any fundamental scientific content or data fabricated using generative AI technologies. To preserve the integrity of scholarly research, the application of AI technology was carried out in conformity with ethical standards and transparency principles.

References

[1] Y Li, J Chen, Y Wang, H Li, J Yin, M Li, L Wang, H Sun and J Chen. Large-scale direct pyrolysis synthesis of excitation-independent carbon dots and analysis of ferric (III) ion sensing mechanism. *Applied Surface Science* 2021; **538**, 148151.

[2] Z Arif, S Sugiarti, E Rohaeti and I Batubara. A Sensor (Optode) Based on Cellulose Triacetate Membrane for Fe(III) Detection in Water Samples. *Chemistry* 2024; **6(1)**, 81-94.

[3] E Piskin, D Cianciosi, S Gulec, M Tomas and E Capanoglu. Iron absorption: Factors, limitations and improvement methods. *ACS Omega* 2022; **7(24)**, 20428-21358.

[4] T Rolić, M Yazdani, S Mandić and S Distante. Iron metabolism, Calcium, Magnesium and Trace elements: A review. *Biological Trace Element Research* 2025; **203**, 2216-2225.

[5] F Liu, Y Jiang, C Fan, L Zhang, Y Hua, C Zhang, N Song, Y Konga and H Wang. Fluorimetric and colorimetric analysis of total iron ions in blood or tap water using nitrogen-doped carbon dots with tunable fluorescence. New *Journal of Chemistry* 2018; **42(12)**, 9676-9683.

[6] H Shumoy and K Raes. Dissecting the facts about the impact of contaminant iron in human nutrition: A review. *Trends in Food Science & Technology* 2021; **116**, 918-927.

[7] J Suebphanpho, A Hasodsong, P Supprung and J Boonmak. Dual-mode luminescence and colorimetric sensing for Al^{3+} and Fe^{2+}/Fe^{3+} ions in water using a zinc coordination polymer. *Spectrochimica Acta Part A: Molecular and Biomolecular Spectroscopy* 2025; **330**, 125729.

[8] P Patil, S Shinde and S Sahoo. Fe^{3+} selective pyrimidine based chromogenic and fluorogenic chemosensor. *Trends in Sciences* 2022; **19(23)**, 4487.

[9] MA Ebrahimzadeh, Z Hashemi and P Biparva. A multifunctional quinoxaline-based chemosensor for colorimetric detection of Fe^{3+} and highly selective fluorescence turn-off response of Cu^{+2} and their practical application. *Spectrochimica Acta Part A: Molecular and Biomolecular Spectroscopy* 2023; **302**, 123092.

[10] B Lal, S Kumar, V Singh, RK Tittal, G Singh, J Singh and VD Ghule. Ampyrone linked 1,2,3-triazole based chemosensor for selective detection of Fe(II and III) ions. *Inorganic Chemistry Communications* 2025; **172**,113692.

[11] Y Tian, J Liu, J Qiao, F Ge, Y Yang and Q Zhang. Advancements in electrochemical sensingTechnology for Heavy Metal Ions Detection. *Food Chemistry: X* 2025; **25**, 102204.

[12] Y Zhou, X Yang, WJ Jang, M Yan and J Yoon. Binding- and activity-based small molecule fluorescent probes for the detection of Cu^{+}, Cu^{2+}, Fe^{2+} and Fe^{3+} in biological systems. *Coordination Chemistry Reviews* 2025; **522**, 216201.

[13] S Baruah, P Hazarika, A Konwar, KK Hazarika and S Hazarika. Synergistic optical sensing of heavy metal ions using Mesua Ferrea derived carbon dot embedded Alginate based biopolymeric film as a sensor platform. *International Journal of Biological Macromolecules* 2025; **286**, 138227.

[14] F Wang, Y Zhang, H Li, W Gong, J Han, S Jiang, D Li and Z Yao. Application of carbon quantum dots as fluorescent probes in the detection of antibiotics and heavy metals. *Food Chemistry* 2025; **463(Part 1)**, 141122.

[15] FK Algethami and HN Abdelhamid. Heteroatoms-doped carbon dots as dual probes for heavy metal detection. *Talanta* 2024; **273**, 125893.

[16] A Kausar. Review multifunctional hybrids of graphene quantum dots with inorganic nanoparticles (Metal, Metal Oxide and MOF) -

topical state and evolutions. *Trends in Sciences* 2025; **22(6)**, 9924.

[17] P Wang, C Chen, H Ren and E Duan. A review of carbon dots in synthesis strategies, photoluminescence mechanisms and applications in wastewater treatment. *Chinese Chemical Letters* 2024; **36(9)**, 110725.

[18] YD Yat, HCY Foo, IS Tan, MK Lam, PL Show and BWL Ng. Synthesis of carbon quantum dots via electrochemically-induced carbon dioxide nanobubbles exfoliation of graphite for heavy metal detection in wastewater. *Journal of Environmental Chemical Engineering* 2024; **12(3)**, 112715.

[19] J Peng, W Gao, BK Gupta, Z Liu, R Romero-Aburto, L Ge, L Song, LB Alemany, X Zhan,G Gao, SA Vithayathil, BA Kaipparettu, AA Marti, T Hayashi, JJ Zhu and PM Ajayan. Graphene quantum dots derived from carbon fibers. *Nano Letters* 2012; **12(2)**, 844-849.

[20] TN Nguyen, PA Le and VBT Phung. Facile green synthesis of carbon quantum dots and biomass-derived activated carbon from banana peels: Synthesis and investigation. *Biomass Conversion and Biorefinery* 2022; **12**, 2407-2416.

[21] X Long and S Wu. Exploring the next super fluorescent carbon Dots: Hydrothermal synthesis of Dual-Function ultra-bright blue fluorescent carbon dots with a quantum yield of 75.4%. *Microchemical Journal* 2024; **207**, 112035.

[22] C Ren, C Tian, M Zhang, F Li, Y Li, F Zhang, J Zhang, G Chen and J Tang. The fluorescence properties of nitrogen-doped carbon dots by microwave green approaches. *Journal of Molecular Structure* 2025; **1319(Part 2)**, 139364.

[23] D Uriarte, C Domini and M Garrido. New carbon dots based on glycerol and urea and its application in the determination of tetracycline in urine samples. *Talanta* 2019; **201**, 143-148.

[24] ZC Yang, M Wang, AM Yong, SY Wong, XH Zhang, H Tan, AY Chang, X Li and J Wang. Intrinsically fluorescent carbon dots with tunable emission derived from hydrothermal treatment of glucose in the presence of monopotassium phosphate. *Chemical Communications* 2011; **47(42)**, 11615-11617.

[25] CEI Torres, TES Quezada, OV Kharissova, H Zeng, BI Kharisov, EL Hipólito, LM Torres-Martínez and LT González. Facile synthesis of hollow carbon fiber/carbon quantum dots composite aerogels for oil sorption. *Geoenergy Science and Engineering* 2023; **231(Part A)**, 212401.

[26] KK Gudimella, T Appidi, HF Wu, V Battula, A Jogdand, AK Rengan and G Gedda. Sand bath assisted green synthesis of carbon dots from citrus fruit peels for free radical scavenging and cell imaging. *Colloids and Surfaces B: Biointerfaces* 2021; **197**, 111362.

[27] PM Sreepian, P Rattanasinganchan and A Sreepian. Antibacterial efficacy of Citrus hystrix (makrut lime) essential oil against clinical multidrug-resistant methicillin-resistant and methicillin-susceptible Staphylococcus aureus isolates. *Saudi Pharmaceutical Journal* 2023; **31(6)**, 1094-1103.

[28] S Srifuengfung, N Bunyapraphatsara, V Satitpatipan, C Tribuddharat, VB Junyaprasert, W Tungrugsasut and V Srisukh. Antibacterial oral sprays from kaffir lime (*Citrus hystrix* DC.) fruit peel oil and leaf oil and their activities against respiratory tract pathogens. *Journal of Traditional and Complementary Medicine* 2020; **10(6)**, 594-598.

[29] N Kooltheat, L Kamuthachad, M Anthapanya, N Samakchan, RP Sranujit, P Potup, A Ferrante and K Usuwanthim. Kaffir lime leaves extract inhibits biofilm formation by Streptococcus mutans. *Nutrition* 2016; **32**, 486-490.

[30] Y Yuandani, AW Septama, LR Nasution, D Dwinanti, DP Rambe, K Ramadhani and WR Manurung. Immunomodulatory effects of citrus species ethanol extracts on cellular immune responses in wistar rats and mice. *Trends in Sciences* 2024; **21(12)**, 8390.

[31] M Lubinska-Szczygieł, A Różańska, J Namieśnik, T Dymerski, RB Shafreen, M Weisz, A Ezra and S Gorinstein. Quality of limes juices based on the aroma and antioxidant properties. *Food Control* 2018; **89**, 270-279.

[32] SB Hussain, CY Shi, LX Guo, HM Kamran, A Sadka and YZ Liu. Recent advances in the regulation of citric acid metabolism in citrus fruit.

Critical Reviews in Plant Sciences 2017; **36(4)**, 241-256.

[33] Y Chen, Y Wu, B Weng, B Wang and C Li. Facile synthesis of nitrogen and sulfur co-doped carbon dots and application for Fe(III) ions detection and cell imaging. *Sensors and Actuators B: Chemical* 2016; **223**, 689-696.

[34] SNAM Yazid, SF Chin, SC Pang and SM Ng. Detection of Sn(II) ions via quenching of the fluorescence of carbon nanodots. *Microchimica Acta* 2013; **180**, 137-143.

[35] D Xu, F Lei, H Chen, L Yin, Y Shi and J Xie. One-step hydrothermal synthesis and optical properties of self-quenching-resistant carbon dots towards fluorescent ink and as nanosensors for Fe^{3+} detection. *RSC Advances* 2019; **9(15)**, 8290-8299.

[36] N Wang, H Chai, X Dong, Q Zhou and L Zhu. Detection of Fe(III)EDTA by using photoluminescent carbon dot with the aid of F^- ion. *Food Chemistry* 2018; **258**, 51-58.

[37] J Yue, L Li, L Cao, M Zan, D Yang, Z Wang, Z Chang, Q Mei, P Miao and WF Dong. Two-Step hydrothermal preparation of carbon dots for calcium ion detection. *ACS Applied Materials & Interfaces* 2019; **11(47)**, 44566-44572.

[38] X Jin and GG Botte. Electrochemical technique to measure Fe(II) and Fe(III) concentrations simultaneously. *Journal of Applied Electrochemistry* 2009; **39**, 1709-1717.

[39] X Gong, W Lu, MC Paau, Q Hu, X Wu, S Shuang, C Dong and MMF Choi. Facile synthesis of nitrogen-doped carbon dots for Fe^{3+} sensing and cellular imaging. *Analytica Chimica Acta* 2015; **861**, 74-84.

[40] N Tirawanchai, K Kengkoom, D Isarangkul, J Burana-osot, T Kanjanapruthipong, S Chantip, P Phattanawasin, U Sotanaphun and S Ampawong. A combination extract of kaffir lime, galangal and lemongrass maintains blood lipid profiles, hepatocytes and liver mitochondria in rats with nonalcoholic steatohepatitis. *Biomedicine & Pharmacotherapy* 2020; **124**, 109843.

[41] D Nugroho, R Benchawattananon, J Janshongsawang, N Pimsin, P Porrawatkul, R Pimsen, P Nuengmatcha, P Nueangmatcha and S Chanthai. Ultra-trace analysis of chromium ions (Cr^{3+}/Cr^{6+}) in water sample using selective fluorescence turn-off sensor with natural carbon dots mixed graphene quantum dots nanohybrid composite synthesis by pyrolysis. *Arabian Journal of Chemistry* 2024; **17(1)**, 105443.

[42] A Iqbal, Y Tian, X Wang, D Gong, Y Guo, K Iqbal, Z Wang, W Liu and W Qin. Carbon dots prepared by solid state method via citric acid and 1,10-phenanthroline for selective and sensing detection of Fe^{2+} and Fe^{3+}. *Sensors and Actuators B: Chemical* 2016; **237**, 408-415.

[43] P Song, L Zhang, H Long, M Meng, T Liu, Y Yin and R Xi. A multianalyte fluorescent carbon dots sensing system constructed based on specific recognition of Fe(III) ions. *RSC Advances* 2017; **7(46)**, 28637-28646.

[44] L Zhao, Y Wang, X Zhao, Y Deng and Y Xia. Facile synthesis of Nitrogen-Doped carbon quantum dots with chitosan for fluorescent detection of Fe^{3+}. *Polymers* 2019; **11(11)**, 1731.

[45] SR Zhang, SK Cai, GQ Wang, JZ Cui and CZ Gao. One-step synthesis of N, P-doped carbon quantum dots for selective and sensitive detection of Fe^{2+} and Fe^{3+} and scale inhibition. *Journal of Molecular Structure* 2021; **1246**, 131173.

[46] X Wang, X. Zu, T Wang, Y Zhao, Y Liang, X Wang, Q Chai, Y Zhang, H Chen and H Wang. N, S-Doped carbon dots prepared by peanut protein isolates and cysteamine as highly sensitive fluorescent sensors for Fe^{2+}, Fe^{3+} and lactoferrin. *Polymers* 2023; **15**, 216.

[47] S Lei, N Chang, J Zhang and H Wang. Dopamine functionalized S, N co-doped carbon dots as a fluorescent sensor for the selective detection of Fe^{3+} and Fe^{2+} in water. *Analytical Sciences* 2021; **37**, 851-857.